

The reflection of narrow slow quantum packets from mirrors

This article has been downloaded from IOPscience. Please scroll down to see the full text article.

2002 J. Phys. A: Math. Gen. 35 8373

(<http://iopscience.iop.org/0305-4470/35/40/302>)

View [the table of contents for this issue](#), or go to the [journal homepage](#) for more

Download details:

IP Address: 171.66.16.109

The article was downloaded on 02/06/2010 at 10:32

Please note that [terms and conditions apply](#).

The reflection of narrow slow quantum packets from mirrors

M A Andreato and V V Dodonov¹

Departamento de Física, Universidade Federal de São Carlos, Via Washington Luiz, km 235, 13565-905 São Carlos, SP, Brazil

E-mail: pmauro@df.ufscar.br and vdodonov@df.ufscar.br

Received 31 October 2001, in final form 4 December 2001

Published 24 September 2002

Online at stacks.iop.org/JPhysA/35/8373

Abstract

We study the reflection of narrow (in space) quantum wavepackets from nonabsorptive mirrors (totally or partially reflecting). If the initial mean value of the momentum component perpendicular to the mirror surface is less than the momentum uncertainty, then the mean value of this component gradually increases with time at the expense of shrinking the packet in the momentum space. As a consequence, very slow particles moving initially in the direction parallel to the mirror surface will be deflected to appreciable angles, even when they pass at macroscopical distances from the mirror. We give analytical expressions describing the *asymptotical behaviour* of wavefunctions and density matrices in the coordinate and momentum representations for arbitrary *narrow* initial packets. We show that the asymptotical mean values and variances do not depend on the phases of the complex reflection and transmission coefficients. Moreover, they are insensitive to the concrete form of the reflective potential in the case of totally reflecting mirrors. For partially reflecting mirrors we introduce the concept of *conditional* wavefunctions and mean values. The dependences of the asymptotical values of different quantities characterizing the packet (e.g. the ‘momentum transformation coefficient’ and the ‘invariant uncertainty product’) on the parameters of the reflecting potential (the height and width or characteristic length of the transition region) are analysed in the examples of the potentials of Epstein’s type and their limit cases (the ideal reflecting wall and the delta potential). A possibility for the verification of the effect of quantum deflection in experiments with ultracold atoms is briefly discussed.

PACS numbers: 03.75.-b, 03.65.-w

¹ On leave from: Lebedev Physics Institute and Moscow Institute of Physics and Technology, Russia.

1. Introduction

Although different aspects of the evolution of quantum wavepackets in free space and in external fields were investigated over the decades [1–14], this subject has not been exhausted yet. Recently the phenomena of reflection and diffraction of *matter waves* from different atomic mirrors or laser beams attracted attention due to the striking progress in experiments with cold atoms [15–21]. However, in all those papers only plane waves or *spatially wide* packets were considered. The aim of our paper is to study the peculiarities of the reflection of *narrow* (in the coordinate space) and *slow* quantum packets from partially reflecting (but nonabsorptive) mirrors. More precisely, we assume that the initial spread of the packet s , its initial mean distance from the boundary x_c and the initial mean velocity v_0 satisfy the conditions $x_c \gg s$ and $v_0 < \hbar/(ms)$ (where m is the mass of the particle). Hitherto the opposite condition $\langle \hat{p}(0) \rangle \gg \sqrt{\sigma_p(0)}$ (where p is the momentum component in the direction perpendicular to the surface and σ_p is the variance of the momentum distribution) was assumed from the very beginning in all studies: see, e.g., [12] and references therein. However, it was shown recently [22] that, for slow narrow packets corresponding to *ultracold particles*, some new interesting effects, such as *quantum deflection* from reflecting mirrors, could be observed.

Suppose that one throws a particle in the direction parallel to the surface of some impenetrable wall. If it were a classical particle, it would not ‘feel’ the presence of the wall at all. But in the quantum case the situation is different due to the ‘wave’ properties of the ‘particle’, represented by some ‘wavepacket’. It is well known that the packet rapidly spreads, so that after some interval of time it will reach the boundary, and eventually all its plane-wave components will be reflected back. As a consequence, the particle will be *deflected* from its initial direction of motion. What is most impressive is the fact that the deflection angle can be made arbitrarily large, depending on the initial velocity and the initial transverse uncertainty of the particle position and, moreover, that it *does not depend on the initial distance* from the boundary [22], which could be quite macroscopical (say, 10 cm, whereas the initial spread of the packet in the transverse direction could be of the order of 10^{-5} cm). This means that the quantum particle ‘feels’ the wall, even when it passes initially very far from it, in the region free of any force. In a wide sense, this is an analogue of the famous Aharonov–Bohm effect, when a charged particle is deflected by a localized magnetic flux, although it travels through a region where there is no magnetic field. Both phenomena have the same origin: quantum nonlocality and the existence of ‘wave properties’ of quantum objects.

In [22] the problem of ‘quantum deflection’ was considered for the model of an ideal wall, equivalent to the boundary condition $\psi(0, t) \equiv 0$, and under several restrictions, such as zero initial mean value of the transverse component of momentum, zero correlation coefficient between the coordinate and momentum in the initial state, and strongly localized initial packet describing a *pure* quantum state. Some of these restrictions were removed in a more detailed study [23], where it was shown explicitly that the effect exists only under the condition $\langle \hat{p}(0) \rangle \ll \sqrt{\sigma_p(0)}$. Nonetheless, since the infinite potential barrier is an idealization, the question remains, whether the effect could exist in the case of realistic mirrors. The main aim of the present paper is to show that the effect of quantum deflection is robust enough against possible nonperfectness of the mirror, as well as against the nonpurity of quantum states.

The plan of the paper is as follows. In section 2 we give analytical expressions describing the *asymptotical behaviour* of *narrow* initial packets (pure and mixed) reflected from arbitrary *nonabsorptive* mirrors, showing that the main characteristics of the effect of deflection are insensitive to the concrete form of the reflective potential in the case of totally reflecting mirrors. For partially reflecting mirrors we introduce the concept of ‘conditional’ wavefunctions and mean values. In section 3 we consider the concrete examples of the Epstein potentials, which

have explicit analytical expressions for the reflection coefficient: the smooth potential step of finite height, the \cosh^{-2} potential and its limit case—the delta potential. Also, an example of a *wide* packet reflected from the ideal boundary shows a qualitative difference in the behaviour of narrow and wide packets. The results of our study are analysed in section 4, where the possibility of verifying the effect in experiments with ultracold atoms is discussed and some new problems to be solved are also pointed out.

2. Reflection of packets from arbitrary nonabsorptive mirrors

In the generic case, the detailed evolution of wavepackets reflected from a non-ideal mirror can be traced only in the framework of approximate or numerical solutions of the Schrödinger equation. However, the *asymptotical* behaviour of initial *narrow* packets can be calculated in practice for any physically reasonable potential.

We suppose that the potential related to the mirror depends only on the coordinate x in the direction perpendicular to the mirror surface. In this case, the mean value of the parallel component of momentum p_z (where z is the coordinate along the surface in the direction of the motion of the particle) does not change with time. If the initial (at $t = 0$) distributions in the x and z directions are uncorrelated, they will remain uncorrelated for $t > 0$ as well. Assuming that the ‘longitudinal’ momentum p_z is defined sufficiently well (i.e. that the part of the initial wavefunction responsible for the z coordinate is close to a plane wave), we may confine ourselves to studying the evolution of the one-dimensional wavefunction $\psi(x, t)$, using the frame moving with the velocity $v_z = p_z/m$ and replacing the time variable t by mz/p_z when interpreting the results in terms of the wavepackets moving in three dimensions (the third space variable, perpendicular to x and z , but also parallel to the surface, is obviously inessential).

We assume for simplicity that the potential describing the mirror is different from zero in a finite domain $-d < x < 0$ (actually, it must decrease sufficiently rapidly outside this domain: see below). A complete set of solutions of the Schrödinger equation in the regions of free motion $x > 0$ and $x < -d$ can be chosen as superpositions of incident and reflected plane waves going to the right and to the left:

$$\psi_k = \frac{e^{-ik^2\tilde{t}}}{\sqrt{2\pi}} \times \begin{cases} e^{-ikx} + \chi(k)e^{ikx}, & x > 0 \\ \zeta(k)e^{-ikx}, & x < -d, \end{cases} \quad (1)$$

$$\psi_{-k} = \frac{e^{-ik^2\tilde{t}}}{\sqrt{2\pi}} \times \begin{cases} \zeta(-k)e^{ikx}, & x > 0 \\ e^{ikx} + \chi(-k)e^{-ikx}, & x < -d, \end{cases} \quad (2)$$

where $k > 0$ and $\tilde{t} \equiv \hbar t/(2m)$. $\chi(k)$ and $\zeta(k)$ are the amplitude reflection and transmission coefficients, respectively, satisfying the condition

$$|\zeta(k)|^2 + |\chi(k)|^2 \equiv 1. \quad (3)$$

The assumption that the motion is free for $x > 0$ and $x < -d$ is not of principal importance, although it permits us to simplify some formulae. Actually, (1) and (2) are *asymptotic* forms of the solution at $x \rightarrow \pm\infty$ for any rapidly decaying potential (the comparison with the exactly solvable models shows that it is sufficient to assume that the potential decays as x^{-2} or faster).

The solutions (1) and (2) are normalized as follows [24]:

$$\int \psi_k(x)\psi_{k'}^*(x) dx = \delta(k - k'), \quad (4)$$

and condition (3) is important for such a normalization. Physically, this condition means the absence of absorption in the mirror. Mathematically, it is equivalent to the *unitarity* of

evolution. The requirement of unitarity results in many identities connecting the reflection and transmission coefficients for positive and negative values of k [25–27]. In particular,

$$\zeta(k) = \zeta(-k), \quad |\chi(k)|^2 = |\chi(-k)|^2, \quad (5)$$

$$\zeta(k)\chi^*(k) + \zeta^*(k)\chi(-k) = 0. \quad (6)$$

The first equality in (5) follows from the reality of the potential, whereas (6) is equivalent to the orthogonality of the states ψ_k and ψ_{-k} .

Using the general formula for the time-dependent propagator of the Schrödinger equation in the form of an integral over a complete set of orthonormal states:

$$G(x, x'; t) = \int_{-\infty}^{\infty} \psi_k(x, t) \psi_k^*(x', 0) dk \quad (7)$$

and expressions (1) and (2), we can write explicit integral representations for the propagator in the regions $x > 0$ and $x < -d$ in terms of the reflection and transmission coefficients. There are four different forms G_{++} , G_{+-} , G_{-+} and G_{--} dependent on the signs of the first and second spatial arguments of the propagator. However, for the packets localized initially totally to the right of the mirror, we need only two forms G_{++} and G_{-+} . Taking into account the identities (3) and (5), one can verify that the part of the propagator $G_{++}(x, x'; t)$ for positive values of x and x' is given by the formula

$$G_{++}(x, x'; t) = \int_0^{\infty} \frac{dk}{2\pi} e^{-ik^2\bar{t}} [e^{ik(x-x')} + e^{-ik(x-x')} + \chi(k)e^{ik(x+x')} + \chi^*(k)e^{-ik(x+x')}]. \quad (8)$$

Using the identity (6) one can also find the part of the propagator $G_{-+}(x, x'; t)$ for $x < -d$ and $x' > 0$:

$$G_{-+}(x, x'; t) = \int_0^{\infty} \frac{dk}{2\pi} e^{-ik^2\bar{t}} [\zeta(k)e^{-ik(x-x')} + \zeta^*(k)e^{ik(x-x')}]. \quad (9)$$

We cannot write an explicit expression for the propagator for $-d < x, x' < 0$ without knowledge of the explicit form of the mirror potential and finding the solutions of the Schrödinger equation for $-d < x < 0$. Hence we cannot calculate the evolution of initial *wide* packets, which were located close to the mirror. Also we cannot follow the evolution of the wavepacket when it reaches the mirror. However, considering initial packets localized far from the mirror, it is sufficient to know the parts of the propagator (8) and (9) to find the *asymptotical behaviour* of the packet, bearing in mind that as $t \rightarrow \infty$, only a negligible part of the packet remains in the vicinity of the mirror (of course, this implies implicitly some limitations on the admissible forms of the mirror potential, such as an absence of bound states, for example).

Applying the propagators (8) and (9) to an initial packet $\psi_0(x')$ localized far to the right from the mirror, one obtains

$$\psi(x > 0, t) = \int_0^{\infty} \frac{dk}{\sqrt{2\pi}} \{e^{ikx} [\varphi_0(k) + \chi(k)\varphi_0(-k)] + e^{-ikx} [\varphi_0(-k) + \chi^*(k)\varphi_0(k)]\} e^{-ik^2\bar{t}}, \quad (10)$$

$$\psi(x < -d, t) = \int_0^{\infty} \frac{dk}{\sqrt{2\pi}} [e^{ikx} \zeta^*(k)\varphi_0(k) + e^{-ikx} \zeta(k)\varphi_0(-k)] e^{-ik^2\bar{t}}, \quad (11)$$

where

$$\varphi_0(k) = \int \frac{dx}{\sqrt{2\pi}} \psi_0(x) e^{-ikx} \quad (12)$$

is the initial wavefunction in the momentum (wavenumber) representation (the integration can be extended to the whole axis, if $\psi_0(x)$ is localized far from the mirror).

When $t \rightarrow \infty$, the part of the integrand in (10) containing the term $\exp(-ikx - ik^2\tilde{t})$ strongly oscillates, due to these oscillations the contribution of this part ‘dies out’. The same happens with the part of the integrand in (11) containing the term $\exp(ikx - ik^2\tilde{t})$. Consequently, asymptotically the coordinate wavefunction tends to the expression

$$\psi_{as}(x, t) = \int_0^\infty \frac{dk}{\sqrt{2\pi}} e^{-ik^2\tilde{t}} \times \begin{cases} [\varphi_0(k) + \chi(k)\varphi_0(-k)]e^{ikx}, & x > 0 \\ \zeta(k)\varphi_0(-k)e^{-ikx}, & x < -d \end{cases} \quad (13)$$

which is nonzero, because the integrands have the stationary points $k_* = |x|/(2\tilde{t})$. The asymptotical wavefunction consists of two packets: one (the first line in the expression above) moves to the right, being located mainly far to the right from the point $x = 0$, and another (the second line) moves to the left, being located far to the left from the point $x = 0$. The ‘tails’ of these packets in the region close to $x = 0$ become negligibly small in the limit $t \rightarrow \infty$. Therefore, calculating the Fourier transform of the function (13) one can extend the limits of integration over dx from $-\infty$ to ∞ for each packet. Then integrals over dx are reduced to delta functions, and we obtain the following asymptotical wavefunction in the momentum representation (remember that $\zeta(k) = \zeta(-k)$):

$$\varphi_{as}(k) = e^{-ik^2\tilde{t}} \times \begin{cases} [\varphi_0(k) + \chi(k)\varphi_0(-k)], & k > 0 \\ \zeta(k)\varphi_0(k), & k < 0. \end{cases} \quad (14)$$

If the initial packet is localized near the ‘central point’ x_c , then one can write

$$\psi_0(x) = \tilde{\psi}_0(x - x_c), \quad \varphi_0(k) = \tilde{\varphi}_0(k) \exp(-ikx_c), \quad (15)$$

where function $\tilde{\varphi}_0(k)$ does not depend on x_c . Therefore

$$\varphi_{as}(k) = e^{-ik^2\tilde{t}} \times \begin{cases} [\tilde{\varphi}_0(k)e^{-ikx_c} + \chi(k)\tilde{\varphi}_0(-k)e^{ikx_c}], & k > 0 \\ \zeta(k)\tilde{\varphi}_0(k)e^{-ikx_c}, & k < 0. \end{cases} \quad (16)$$

The asymptotical momentum distribution $\mathcal{P}_{as}(k) = |\varphi_{as}(k)|^2$ for $k > 0$ is

$$\mathcal{P}_{as}(k) = |\tilde{\varphi}_0(k)|^2 + |\tilde{\varphi}_0(-k)|^2 + 2 \operatorname{Re}[\tilde{\varphi}_0^*(k)\tilde{\varphi}_0(-k)\chi(k)e^{2ikx_c}]. \quad (17)$$

The last term in (17) depends on the initial position of the packet and it strongly oscillates when $x_c \rightarrow \infty$. But this strongly oscillating term cannot affect the observable integral characteristics of the packet, such as the asymptotical mean momentum or the momentum dispersion, if initially the packet was far enough from the mirror (because the argument of the exponential function kx_c has an order of $x_c/s \gg 1$ in the region of k space which yields the main contribution to the integrals containing $\mathcal{P}_{as}(k)$, where s is the initial characteristic width of the packet in the coordinate space). Hence in the asymptotical regime one can use a simplified averaged (nonoscillating) distribution

$$\overline{\mathcal{P}}_{as}(k) = \begin{cases} |\tilde{\varphi}_0(k)|^2 + |\chi(k)\tilde{\varphi}_0(-k)|^2, & k > 0 \\ |\zeta(k)\tilde{\varphi}_0(k)|^2, & k < 0. \end{cases} \quad (18)$$

Note that the asymptotical momentum distribution depends only on *absolute values* of the reflection and transmission coefficients and not on their phases.

For totally reflecting mirrors ($\zeta(k) \equiv 0$, i.e. for potentials going to ∞ as $x \rightarrow -\infty$) the averaged asymptotical momentum distribution is

$$\overline{\mathcal{P}}_{as}(k) = \begin{cases} 0, & k < 0 \\ |\tilde{\varphi}_0(k)|^2 + |\tilde{\varphi}_0(-k)|^2, & k > 0, \end{cases} \quad (19)$$

and it depends neither on the initial position of the packet nor on the characteristics of a totally reflecting mirror (i.e. on the concrete form of the reflecting potential $V(x)$ or the phase of the

reflection coefficient $\chi(k)$). For any totally reflecting mirror the asymptotical mean value of the wavenumber is the same as in the case of the ideal mirror studied in detail in [22, 23]:

$$\langle k_\infty \rangle_{\mathcal{W}} = \int_0^\infty k[|\tilde{\varphi}_0(k)|^2 + |\tilde{\varphi}_0(-k)|^2] dk, \quad (20)$$

where the suffix \mathcal{W} means the case of an ideal impenetrable *wall*. The initial mean value is

$$\langle k(0) \rangle = \int_{-\infty}^\infty k|\tilde{\varphi}_0(k)|^2 dk = \int_0^\infty k[|\tilde{\varphi}_0(k)|^2 - |\tilde{\varphi}_0(-k)|^2] dk, \quad (21)$$

whereas

$$\langle k_\infty^2 \rangle = \langle k^2(0) \rangle = \int_0^\infty k^2[|\tilde{\varphi}_0(k)|^2 + |\tilde{\varphi}_0(-k)|^2] dk. \quad (22)$$

The concrete form of the totally reflecting potential is important only for the knowledge of the details of evolution in the intermediate regime (e.g. the time of approaching the asymptotical state) and the details of oscillations in the exact (unaveraged) distributions, such as (17).

2.1. Momentum transformation coefficient

If the initial momentum distribution is localized near some negative value $-|k_0| \sim \langle k(0) \rangle$, then the asymptotical distribution has practically the same form, but it is localized nearby $|k_0|$, so that $\langle k_\infty \rangle_{\mathcal{W}} \approx -\langle k(0) \rangle$. However, if $|k_0|$ is less than the spread of the initial momentum distribution $\sqrt{\sigma_k}$, then the form of the final distribution differs significantly from the initial one, and $\langle k_\infty \rangle_{\mathcal{W}}$ can be quite different from $|\langle k(0) \rangle|$, especially if the last quantity is close to zero. The changes of the absolute value of the mean momentum and the width of the momentum distribution function can be characterized quantitatively by the ‘mean momentum transformation coefficient’ η and the ‘momentum variance transformation coefficient’ τ , respectively:

$$\eta \equiv \frac{\langle \hat{p}(\infty) \rangle^2 - \langle \hat{p}(0) \rangle^2}{\langle \hat{p}^2(0) \rangle}, \quad \tau \equiv \frac{\sigma_p(0) - \sigma_p(\infty)}{\sigma_p(0)} = \frac{\langle \hat{p}(\infty) \rangle^2 - \langle \hat{p}(0) \rangle^2}{\sigma_p(0)}. \quad (23)$$

Consider, for example, the initial narrow *Gaussian* packet:

$$|\psi(x, 0)|^2 = (\pi s^2)^{-1/2} \exp[-(x - x_c)^2/s^2], \quad x_c \gg s, \quad (24)$$

$$|\tilde{\varphi}_0(\tilde{k})|^2 = \pi^{-1/2} \exp[-(\tilde{k} - k_0)^2], \quad \tilde{k} = ps/(m\hbar). \quad (25)$$

In this case

$$\langle \tilde{k}(\infty) \rangle = \pi^{-1/2} \exp(-2k_0^2) + k_0 \operatorname{erf}(k_0), \quad (26)$$

where the error function is defined as [28]

$$\operatorname{erf}(z) = 2\pi^{-1/2} \int_0^z \exp(-y^2) dy. \quad (27)$$

Both coefficients, η and τ , rapidly go to zero if $|k_0| \gg 1$ (note that (26) is an even function of k_0):

$$\eta \approx -\frac{2 \exp(-k_0^2)}{|k_0| \sqrt{\pi}}, \quad \tau \approx -\frac{4|k_0|}{\sqrt{\pi}} e^{-k_0^2}, \quad |k_0| \gg 1.$$

The change of the absolute value of the momentum for the Gaussian states is maximal for $k_0 = 0$, when $\tau = \eta = \eta_* = 2/\pi \approx 0.64$. However, choosing proper initial states, one can obtain the values of η and τ arbitrarily close to 1 (for the totally reflecting boundary).

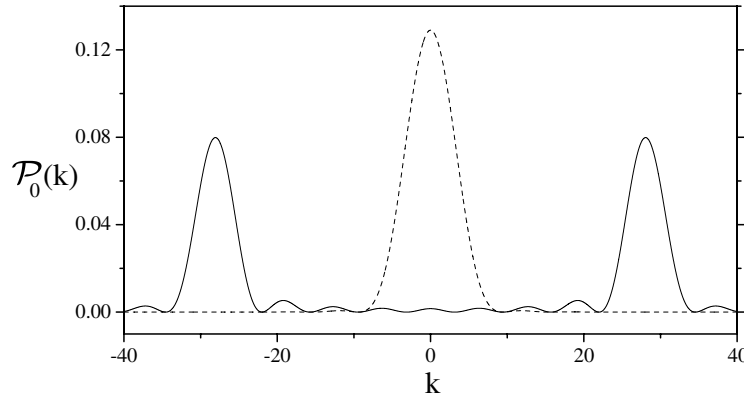


Figure 1. The initial momentum distribution for the ‘waveguide’ packets (29) with $n = 1$ (broken curve) and $n = 9$ (full curve); $k_0 = 0, s = 1$.

Suppose that the particle left some atomic trap passing inside a long planar waveguide of width s . Then the initial coordinate wavefunction $\tilde{\psi}_0(y)$ has the form (for odd modes, $n = 1, 3, 5, \dots$)

$$\tilde{\psi}_0(y) = \begin{cases} \sqrt{(2/s)} e^{ik_0 y} \cos(n\pi y/s), & |y| < s/2, \\ 0, & |y| > s/2, \end{cases} \quad (28)$$

so that the initial momentum distribution depends on the wavenumber k as

$$\mathcal{P}_0(k) = \frac{4\pi s n^2 \cos^2[s(k - k_0)/2]}{[(n\pi)^2 - s^2(k - k_0)^2]^2}, \quad \langle \hat{k}(0) \rangle = k_0, \quad \sigma_k(0) = (n\pi/s)^2. \quad (29)$$

For $k_0 = 0$ and $n \gg 1$, the function (29) has high and sharp maxima at $k_n = \pm n\pi/s$ (the ratio $\mathcal{P}(k_n)/\mathcal{P}(0)$ equals $\pi^2 n^2/16$, whereas the width of the peak is of the order of π/s : see figure 1). The asymptotical value of the mean momentum equals

$$\begin{aligned} \langle k(\infty) \rangle &= \frac{1}{\pi^2 n s} \{ (n\pi)^2 [\text{Si}(n\pi - k_0 s) + \text{Si}(n\pi + k_0 s)] \\ &\quad + n\pi k_0 s [\text{Si}(n\pi + k_0 s) - \text{Si}(n\pi - k_0 s)] \\ &\quad + k_0 s [\text{Cin}(n\pi + k_0 s) - \text{Cin}(n\pi - k_0 s)] - 2n\pi [1 + \cos(k_0 s)] \}, \end{aligned} \quad (30)$$

$$\text{Cin}(z) = \int_0^z \frac{1 - \cos(t)}{t} dt, \quad \text{Si}(z) = \int_0^z \frac{\sin(t)}{t} dt.$$

The momentum transformation coefficient η (23) is maximal for $k_0 = 0$, when

$$\langle k(\infty) \rangle = \frac{2}{\pi^2 n s} [(n\pi)^2 \text{Si}(n\pi) - 2n\pi].$$

For $n \gg 1$, $\text{Si}(n\pi) = \pi/2 + 1/(n\pi) + \dots$, n odd, and the coefficient η can be made as close to unity as desired:

$$\langle k(\infty) \rangle = \frac{n\pi}{s} \left[1 - \frac{2}{n\pi^2} + \dots \right], \quad \eta_{max} = 1 - \frac{4}{n\pi^2} + \dots$$

In contrast, if $|k_0|s/(n\pi) \gg 1$, then equation (30) yields $\langle k(\infty) \rangle = |k_0| + \mathcal{O}(k_0^{-2})$, so that $\tau \sim |k_n/k_0|$ and $\eta \sim |k_n/k_0|^3$. In the case of even waveguide modes we have similar relations: one should replace \cos by \sin in equations (28) and (29), and change the sign before \cos in the last line of equation (30), taking $n = 2, 4, \dots$. The dependence of the momentum transformation coefficient (23) on the normalized initial mean momentum,

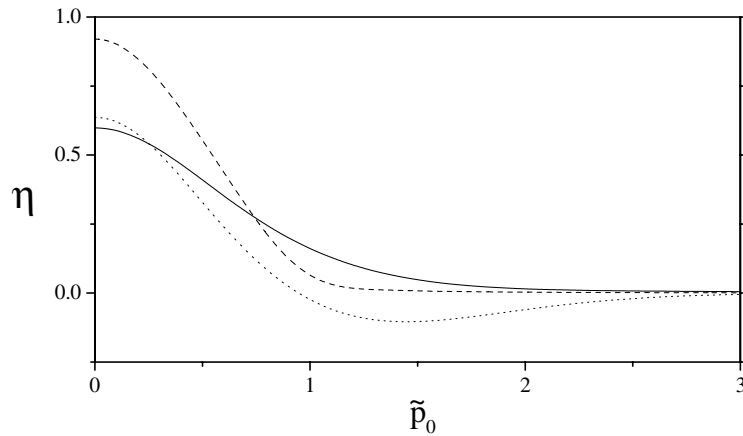


Figure 2. The momentum transformation coefficient (23) versus the normalized initial mean momentum, $\tilde{p}_0 \equiv \langle \hat{p}(0) \rangle / [\sigma_p(0)]^{1/2}$, for different initial localized states: Gaussian packet (24) (dotted curve assuming negative values for $\tilde{p}_0 > 1$), ‘waveguide’ packet (29) with $n = 1$ (full curve) and ‘waveguide’ packet (29) with $n = 5$ (broken curve).

$\tilde{p}_0 \equiv \langle \hat{p}(0) \rangle / \sqrt{\sigma_p(0)}$, for different initial states is shown in figure 2. It is clearly seen that significant changes of the momentum distribution, resulting in a significant deflection, can be observed only for $\tilde{p}_0 \ll 1$.

2.2. Partially reflecting mirrors: standard and ‘conditional’ mean values

For a partially reflecting mirror, there is a nonzero asymptotical probability to find the particle to the left from the barrier $\int_{-\infty}^{-d} |\psi_{as}(x)|^2 dx$. Using equation (13) for $\psi_{as}(x)$ in the region $x < -d$, we can formally extend the integration over dx to $+\infty$, because the added region does not contribute to the integral in the limit $t \rightarrow \infty$. Thus we arrive at the expressions for the total asymptotical probabilities of finding the particle to the left (\mathcal{L}) and to the right (\mathcal{R}) from the barrier (mirror), which have a clear physical interpretation:

$$\mathcal{L} = \int_0^{\infty} |\zeta(k)|^2 |\tilde{\varphi}_0(-k)|^2 dk = 1 - \mathcal{R}, \quad (31)$$

$$\mathcal{R} = \int_0^{\infty} [|\tilde{\varphi}_0(k)|^2 + |\chi(k)|^2 |\tilde{\varphi}_0(-k)|^2] dk. \quad (32)$$

For partially reflecting mirrors we have

$$\langle k_{\infty} \rangle = \int_0^{\infty} k dk [|\tilde{\varphi}_0(k)|^2 + (|\chi(k)|^2 - |\zeta(k)|^2) |\tilde{\varphi}_0(-k)|^2], \quad (33)$$

whereas $\langle k_{\infty}^2 \rangle$ still equals $\langle k^2(0) \rangle$. Formula (33) is an easily verified consequence of the standard definition of the mean value $\langle k_{\infty} \rangle = \int_{-\infty}^{\infty} k \overline{\mathcal{P}}_{as}(k) dk$. However, this definition, where integration is performed over *all points* in the momentum (or, equivalently, coordinate) space from $-\infty$ to $+\infty$, is based on the implicit assumption that one can perform measurements of the observables in the asymptotical state in *any region* of the coordinate and momentum spaces, in particular in the region $x < -d$ *behind the mirror*. One can imagine another situation, when only the semispace $x > 0$ is accessible for experiments (actually, it seems even more adequate in the case of experiments with cold atoms, when a particle striking the mirror and passing through it or absorbed by it is lost for the further measurements).

In such a case, the asymptotical state is described by the part of the total wavefunction given in the first line on the right-hand side of equation (13) in the coordinate representation and by the first line of equation (14) in the momentum representation. Obviously, these reduced functions must be renormalized by dividing them by the factor $\sqrt{\mathcal{R}}$ (32). If \mathcal{R} is significantly different from 1, then the ‘conditional’ mean values of observables calculated with the aid of the reduced probabilities (we shall supply them with a suffix \mathcal{R}) turn out to be quite different from the ‘unconditional’ ones²:

$$\langle k_\infty^n \rangle_{\mathcal{R}} = \frac{1}{\mathcal{R}} \int_0^\infty k^n dk [|\tilde{\varphi}_0(k)|^2 + |\chi(k)|^2 |\tilde{\varphi}_0(-k)|^2]. \tag{34}$$

The difference between unconditional and conditional mean values becomes significant for weakly reflecting mirrors, when $|\chi(k)| \ll 1$ for those values of k which yield the main contribution to the integrals. For example, for symmetrical initial distribution $\tilde{\varphi}_0(k) = \tilde{\varphi}_0(-k)$, the unconditional momentum transformation coefficient η (23) is small. Under the same conditions, \mathcal{R} is close to 1/2, therefore $\langle k_\infty \rangle_{\mathcal{R}} \approx \langle k_\infty \rangle_{\mathcal{W}}$. Hence the conditional transformation coefficient is approximately the same as in the case of an ideal boundary. If initially $\tilde{\varphi}_0(k) \ll \tilde{\varphi}_0(-k)$ for $k > 0$ (i.e. the particle approaches the mirror), then obviously $\mathcal{R} \ll 1$ for $|\chi(k)| \ll 1$. In this case $\langle k_\infty \rangle \approx \langle k(0) \rangle < 0$, while $\langle k_\infty \rangle_{\mathcal{R}}$ is positive.

Consider, for the sake of simplicity, a *symmetrical* and *real* initial distribution $\tilde{\varphi}_0(k) = \tilde{\varphi}_0(-k)$, which ensures the zero value of the initial mean momentum. Calculating the mean values in the momentum representation with the aid of the wavefunction (16), we obtain the following leading terms for $t \rightarrow \infty$ (the omitted terms either decrease at least as t^{-1} or they are much less than time-independent terms preserved in the expressions below):

$$\langle x \rangle = \hbar \langle k_\infty \rangle t / m + 2x_c \mathcal{L}, \quad \langle x^2 \rangle = \hbar^2 \langle k^2 \rangle t^2 / m^2 + x_c^2, \tag{35}$$

$$\langle \hat{x} \hat{p} + \hat{p} \hat{x} \rangle = 2\hbar^2 \langle k^2 \rangle t / m, \tag{36}$$

where³

$$\langle k_\infty \rangle = 2 \int_0^\infty k |\chi(k)|^2 |\tilde{\varphi}_0(k)|^2 dk, \quad \langle k^2 \rangle = 2 \int_0^\infty k^2 |\tilde{\varphi}_0(k)|^2 dk. \tag{37}$$

Calculating the *conditional* mean values we obtain the following expressions:

$$\langle x \rangle_{\mathcal{R}} = \hbar \langle k_\infty \rangle_{\mathcal{R}} t / m + x_c \frac{\mathcal{L}}{\mathcal{R}}, \quad \langle x^2 \rangle_{\mathcal{R}} = \hbar^2 \langle k^2 \rangle_{\mathcal{R}} t^2 / m^2 + x_c^2 + 2\hbar x_c t \Theta / m, \tag{38}$$

$$\langle \hat{x} \hat{p} + \hat{p} \hat{x} \rangle_{\mathcal{R}} = 2\hbar^2 \langle k^2 \rangle_{\mathcal{R}} t / m + \hbar x_c \Theta, \tag{39}$$

where

$$\langle k_\infty^n \rangle_{\mathcal{R}} = \frac{1}{\mathcal{R}} \int_0^\infty k^n (1 + |\chi(k)|^2) |\tilde{\varphi}_0(k)|^2 dk, \quad n = 1, 2, \tag{40}$$

$$\Theta = \frac{1}{\mathcal{R}} \int_0^\infty k |\zeta(k)|^2 |\tilde{\varphi}_0(k)|^2 dk = \frac{\langle k_\infty \rangle_{\mathcal{W}}}{\mathcal{R}} - \langle k_\infty \rangle_{\mathcal{R}}. \tag{41}$$

² Similar ideas were discussed in [29] in connection with the tunnelling problem. However, the ‘conditional probabilities’ introduced in [29] were complex in the generic case.

³ Remember that in the momentum representation the coordinate operator is $\hat{x} = i\partial/\partial k$. If one calculated only derivatives of the exponential functions in (16), then imaginary terms in the second-order moments could appear at first glance. However, these terms are cancelled if one takes into account the terms $\partial\tilde{\varphi}_0(k)/\partial k$. Since reflection and transmission coefficients do not depend on x_c , their derivatives with respect to k give corrections which are small compared with terms proportional to time or x_c .

2.3. Asymptotical density matrices of mixed quantum states

Until now, we considered *pure* quantum states described in terms of the wavefunction. But the states created in real experiments are hardly perfectly pure: soon they are *quantum mixtures* described in terms of the density matrices $\rho(x, x') = \rho^*(x', x)$. Their evolution is governed by the double integral

$$\rho(x, x', t) = \iint G(x, y, t)G^*(x', y', t)\rho(y, y', 0) dy dy'. \quad (42)$$

The calculations in this case are more tedious than for pure states, but the final result is quite expected: it is enough to replace formally the product $\psi_{as}(x)\psi_{as}^*(x')$ by $\rho_{as}(x, x')$. For $x, x' > 0$ we obtain

$$\begin{aligned} \rho_{as}^{++}(x, x', t) &= \int_0^\infty \frac{dk dk'}{2\pi} \exp[i(kx - k'x') - i\tilde{t}(k^2 - k'^2)] \\ &\times [\chi(k)\rho_0(-k, k') + \chi^*(k')\rho_0(k, -k') + \rho_0(k, k') + \chi(k)\chi^*(k')\rho_0(-k, -k')]. \end{aligned}$$

The Fourier transform of $\rho(x, x')$ gives the density matrix in the momentum representation

$$\rho(k, k', t) = \int \frac{dx dx'}{2\pi} \rho(x, x', t) \exp[-i(kx - k'x')]. \quad (43)$$

The initial density matrices localized near the central point x_c can be written as

$$\rho_0(x, x') = \tilde{\rho}_0(x - x_c, x' - x_c), \quad \rho_0(k, k') = \tilde{\rho}_0(k, k') \exp[-ix_c(k - k')],$$

where the function $\tilde{\rho}_0(k, k')$ does not depend on x_c . Making the same approximations as in the preceding subsections, and suppressing strongly oscillating terms proportional to $\exp[\pm ix_c(k + k')]$ with $kk' > 0$, we find the averaged asymptotical density matrices

$$\begin{aligned} \bar{\rho}_{as}^{++}(k, k', t) &= \exp[-i\tilde{t}(k^2 - k'^2)]\{\tilde{\rho}_0(k, k') \exp[-ix_c(k - k')] \\ &+ \chi(k)\chi^*(k')\tilde{\rho}_0(-k, -k') \exp[-ix_c(k' - k)]\}, \end{aligned} \quad (44)$$

$$\bar{\rho}_{as}^{--}(k, k', t) = \zeta(k)\zeta^*(k')\tilde{\rho}_0(k, k') \exp[-i\tilde{t}(k^2 - k'^2) - ix_c(k - k')], \quad (45)$$

where the superscripts give the signs of the first and second arguments. We see that the *diagonal elements* do not depend on the phases of the coefficients $\chi(k)$ and $\zeta(k)$ (we do not bring the expressions for $\bar{\rho}_{as}^{+-}(k, k', t)$ and $\bar{\rho}_{as}^{-+}(k, k', t)$ because they do not contribute to the diagonal elements).

3. Examples: reflection of Gaussian packets

The effect of quantum deflection was discovered in [22] and studied in [23] in the framework of the analysis of exact solutions of the time-dependent Schrödinger equation in the presence of an ideal boundary. One could have some doubts concerning the physical meaning of such a model, believing it to be oversimplified. Indeed, the ideal wall potential possesses two unrealistic features: it has an infinite height and zero extension of the transition region. In this section, using the general formulae derived in the preceding section, we analyse two families of smooth potentials with finite heights, demonstrating explicitly that the model of ideal boundary is the well defined limit of more realistic potentials. The first family describes smooth potential steps, which can be considered as the models of sufficiently *thick* barriers (mirrors):

$$V_1(x) = V_0/(1 + e^{x/w}). \quad (46)$$

The second potential can be treated as a model of a *thin* mirror:

$$V_2(x) = V_0/\cosh^2(x/w). \quad (47)$$

Our choice is explained by two circumstances. Firstly, both potentials are the special cases of the known family of Epstein’s potentials [30] admitting exact solutions of the stationary Schrödinger equation [24, 31]. Secondly, both potentials have exponential ‘tails’, which is a typical feature of the ‘evanescent mirrors’ frequently used in the experiments with ultracold atoms [19, 21, 32–35].

In the preceding section we have seen that the momentum transformation coefficient is essentially different from zero only under the condition $\langle \hat{p}(0) \rangle \ll \sqrt{\sigma_p(0)}$, we shall consider hereafter the case of $\langle \hat{p}(0) \rangle = 0$. Moreover, we confine ourselves to a simple example of the initial mixed *Gaussian* state with *real* parameters, which has zero initial average momentum and zero initial correlation coefficient between the coordinate and momentum (the influence of this correlation coefficient was studied in [23] in the special case of an ideal wall):

$$\rho(y, y', 0) = \frac{1}{s\sqrt{\pi}} \exp\left\{-\frac{1}{s^2}\left[\frac{y^2 + y'^2}{2(1-\lambda)} - \frac{\lambda yy'}{1-\lambda} - x_c(y+y') + x_c^2\right]\right\}, \quad (48)$$

where s is the initial width of the packet in the coordinate space, x_c is its initial mean position and the parameter λ ($0 \leq \lambda < 1$) is responsible for the quantum impurity (which is conserved in time in the absence of dissipation):

$$\mathcal{C} \equiv \text{Tr } \hat{\rho}^2 = \sqrt{\frac{1-\lambda}{1+\lambda}}, \quad \langle \tilde{p}^2(0) \rangle = \sigma_p(0) = \frac{\hbar^2}{2s^2\mathcal{C}^2}. \quad (49)$$

The state (48) possesses the *symmetrical* momentum distribution

$$\rho_0(\tilde{p}, \tilde{p}) = \pi^{-1/2} \exp(-\tilde{p}^2) = \rho_0(-\tilde{p}, -\tilde{p}), \quad \tilde{p} = ps\mathcal{C}/\hbar. \quad (50)$$

The specific feature of the Gaussian distribution is that the ‘purity’ \mathcal{C} can be included in the definition of the scaled dimensionless momentum variable \tilde{p} . For the symmetrical distributions, the formulae for the mean values and the probability of staying to the right of the barrier can be simplified as follows:

$$\langle k_\infty \rangle = 2 \int_0^\infty k \, dk \, |\chi(k)|^2 \rho_0(k, k), \quad (51)$$

$$\langle k_\infty \rangle_{\mathcal{R}} = \frac{1}{\mathcal{R}} \int_0^\infty k \, dk \, (1 + |\chi(k)|^2) \rho_0(k, k), \quad (52)$$

$$\langle k_\infty^2 \rangle = 2 \int_0^\infty k^2 \, dk \, \rho_0(k, k), \quad (53)$$

$$\langle k_\infty^2 \rangle_{\mathcal{R}} = \frac{1}{\mathcal{R}} \int_0^\infty k^2 \, dk \, (1 + |\chi(k)|^2) \rho_0(k, k), \quad (54)$$

$$\mathcal{R} = \frac{1}{2} + \int_0^\infty |\chi(k)|^2 \rho_0(k, k) \, dk. \quad (55)$$

3.1. Potential steps

In the case of potential (46) the reflection coefficient depends on the scaled variable \tilde{p} as [24,31] ($k > 0$)

$$|\chi_1(\tilde{p})|^2 = \begin{cases} 1, & \tilde{p}^2 \leq \kappa \\ \left| \frac{\sinh[\pi\alpha(\tilde{p} - \sqrt{\tilde{p}^2 - \kappa})]}{\sinh[\pi\alpha(\tilde{p} + \sqrt{\tilde{p}^2 - \kappa})]} \right|^2, & \tilde{p}^2 \geq \kappa \end{cases}, \quad (56)$$

where

$$\kappa \equiv 2mV_0s^2\mathcal{C}^2/\hbar^2, \quad \alpha \equiv w/(s\mathcal{C}). \quad (57)$$

The momentum transformation coefficient (23) for the potential (46) is

$$\eta_1 = \frac{2}{\pi} \left(1 - e^{-\kappa} + \int_{\kappa}^{\infty} \left| \frac{\sinh[\pi\alpha(\sqrt{z} - \sqrt{z - \kappa})]}{\sinh[\pi\alpha(\sqrt{z} + \sqrt{z - \kappa})]} \right|^2 e^{-z} dz \right)^2. \quad (58)$$

Formally, the infinitely high potential wall corresponds to $\kappa = \infty$. However, already for $\kappa \approx 1$ (i.e. if the barrier is only two times higher than the mean energy of the packet $\langle \tilde{p}^2(0) \rangle / (2m)$) the coefficient η equals about 50% of its maximal value $\eta_* = 2/\pi$, and $|\eta_* - \eta|/\eta_* < 10\%$ for $\kappa > 3$, *independently of the parameter α* characterizing the ‘sharpness’ of the potential.

3.2. ‘Thin mirror’ model

In the case of a ‘thin-mirror’ potential (47) the reflection coefficient is less than 1 for any value of the dimensionless momentum \tilde{p} [24]:

$$|\chi_2(\tilde{p})|^2 = \frac{\mathcal{A}}{\mathcal{A} + \sinh^2(\pi\alpha\tilde{p})}, \quad \mathcal{A} = \cos^2\left(\frac{\pi}{2}\sqrt{1 - 4\kappa\alpha^2}\right), \quad (59)$$

where α and κ are the same as in equation (57). If the argument of the square root in the definition of the coefficient \mathcal{A} is negative, then \cos should be replaced by \cosh . The momentum transformation coefficient is

$$\eta_2 = \frac{2}{\pi} \left| \int_0^{\infty} \frac{\mathcal{A}e^{-z} dz}{\mathcal{A} + \sinh^2(\pi\alpha\sqrt{z})} \right|^2. \quad (60)$$

If α is of the order of unity (or larger) and $\kappa > 1$, then $\mathcal{A} \approx \cosh^2(\pi\alpha\sqrt{\kappa})$. Due to the factor e^{-z} in the integrand of (60), the main contribution to the integral is given by the interval $0 < z < z_* \sim 1$. If the ratio κ/z_* exceeds the unit value, then $\mathcal{A}/[\mathcal{A} + \sinh^2(\pi\alpha\sqrt{z})] \approx 1$ for $0 < z < z_*$, and the integral is close to 1, *again independently of α* .

Typical dependences of the mean momentum transformation coefficient (23) on the dimensionless height of the potentials κ for the fixed values of the dimensional width α are given in figure 3. Two upper curves correspond to the step potential (46), whose widths differ by four orders of magnitude: $\alpha = 0.001$ (sharp potential step) and $\alpha = 10$. Nonetheless, both curves are very close for any value of κ . Moreover, for $\kappa > 4$ the parameter η becomes very close to the maximal value $2/\pi$ corresponding to the infinitely high and sharp potential wall. Four lower curves correspond to the ‘pulse-like’ potential (47) (note the ‘inverse’ order of curves with respect to the potential step case). If the ‘thickness’ of the barrier is of the order of the initial spread of the packet (48) in the coordinate space ($\alpha \sim 1$) or larger, then the coefficient η becomes close to the limit value for $\kappa > 4$, as well as in the potential step case. For $\alpha = 10$ (and greater) the curves corresponding to the potentials (46) and (47) become practically indistinguishable: see the bold curve (the second from the top).

3.3. Delta-potential

In the case of ‘very thin’ potentials with $\alpha \ll 1$, the properties of the reflected packets depend, as a matter of fact, on the single parameter $\mathcal{K} \equiv (\kappa\alpha)^2$. Indeed, for $\alpha \ll 1$ and $\kappa\alpha^2 \ll 1$, and for not too large values of \tilde{p} , $\tilde{p} \sim \mathcal{O}(1)$ (which give the main contribution to all integral characteristics of the packet), one can simplify the expressions in equation (59), obtaining the following reflection and transmission coefficients:

$$|\chi(\tilde{p})|^2 = \frac{\mathcal{K}}{\mathcal{K} + \tilde{p}^2}, \quad |\zeta(\tilde{p})|^2 = \frac{\tilde{p}^2}{\mathcal{K} + \tilde{p}^2}. \quad (61)$$

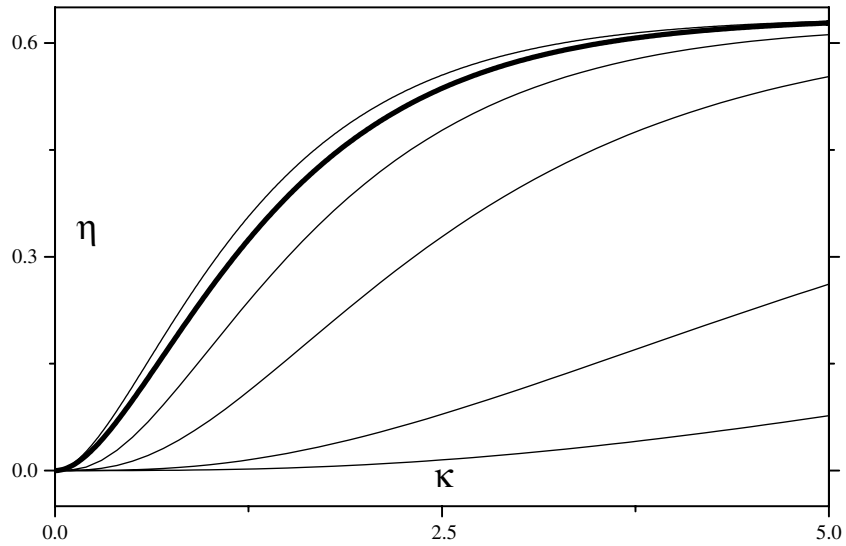


Figure 3. The momentum transformation coefficient (23) versus the dimensionless height of the potentials κ for several fixed values of the dimensionless width α , for the Gaussian packet (50) and two different potentials. Four lower curves correspond to the ‘pulse-like’ potential (47). The values of the parameter α are as follows (from the bottom to the top): 0.1, 0.2, 0.5, 1.0. The bold curve (the fifth from the bottom or the second from the top) corresponds to $\alpha = 10$, and it is common for the potential (47) and the ‘step’ potential (46) (with the same value of α). The uppermost curve corresponds to the step potential with $\alpha = 0.001$.

On the other hand, the expressions in (61) exactly coincide with the reflection and transmission coefficients for the *delta potential* [31, 36]:

$$V(x) = \mathcal{Z}\delta(x), \tag{62}$$

if one identifies $\mathcal{Z} = 2V_0w$, so that $\mathcal{K} = (ms\mathcal{Z}C/\hbar^2)^2$. Therefore, the delta potential can be used as a good simple approximation of very thin barriers (actually, this potential is frequently used to model quite different phenomena in various fields of quantum physics: see, e.g., [37] for one of the most recent reviews). Note that the coefficient \mathcal{K} does not depend on the sign of the potential strength \mathcal{Z} , which means that the repulsive and attractive delta potentials give rise to the same asymptotical probabilities and mean values.

We use the advantage of simple formulae (61) to analyse the difference between the ‘conditional’ and ‘unconditional’ mean values introduced in section 2.2. Calculating the integrals (51)–(55) we obtain the following expressions:

$$\langle \tilde{p}_\infty \rangle = \frac{f(\mathcal{K})}{\sqrt{\pi}}, \quad \langle \tilde{p}_\infty \rangle_{\mathcal{R}} = \frac{1}{\sqrt{\pi}} \frac{1 + f(\mathcal{K})}{1 + g(\mathcal{K})}, \quad \langle \tilde{p}_\infty^2 \rangle_{\mathcal{R}} = \frac{1 + 2\mathcal{K}[1 - g(\mathcal{K})]}{2[1 + g(\mathcal{K})]},$$

$$f(\mathcal{K}) = \mathcal{K} \exp(\mathcal{K})E_1(\mathcal{K}), \quad g(\mathcal{K}) = 2\mathcal{R} - 1 = \sqrt{\pi\mathcal{K}} \exp(\mathcal{K})\text{erfc}(\sqrt{\mathcal{K}}).$$

Here

$$E_1(x) = \int_1^\infty \frac{dt}{t} \exp(-xt) = \int_x^\infty \frac{dt}{t} \exp(-t) \tag{63}$$

is the integral exponential function [38] and

$$\text{erfc}(z) = \frac{2}{\sqrt{\pi}} \int_z^\infty \exp(-y^2) dy \equiv 1 - \text{erf}(z) \tag{64}$$

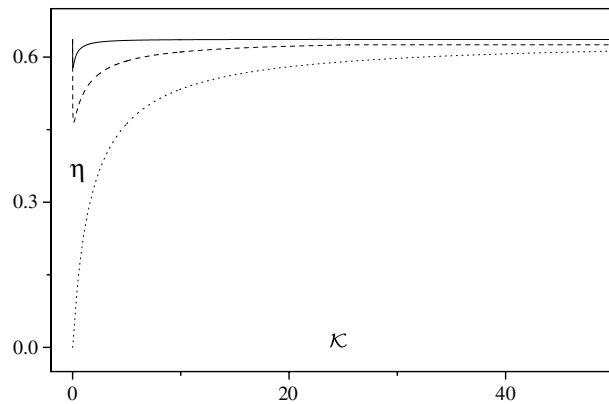


Figure 4. Three different momentum transformation coefficients (66) versus the scaled normalized delta-potential strength \mathcal{K} . The order of the curves from bottom to top: unconditional coefficient η ; conditional coefficient $\eta_{\mathcal{R}}$; conditional coefficient $\eta'_{\mathcal{R}}$.

is the complementary error function [39]. The momentum transformation coefficients

$$\eta = \langle \tilde{p}_{\infty} \rangle^2 / \langle \tilde{p}^2(0) \rangle, \quad \eta_{\mathcal{R}} = \langle \tilde{p}_{\infty} \rangle_{\mathcal{R}}^2 / \langle \tilde{p}^2(0) \rangle, \quad \eta'_{\mathcal{R}} = \langle \tilde{p}_{\infty} \rangle_{\mathcal{R}}^2 / \langle \tilde{p}_{\infty} \rangle_{\mathcal{R}} \quad (65)$$

depend only on \mathcal{K} :

$$\eta = \frac{2}{\pi} [f(\mathcal{K})]^2, \quad \eta_{\mathcal{R}} = \frac{2}{\pi} \left[\frac{1 + f(\mathcal{K})}{1 + g(\mathcal{K})} \right]^2, \quad \eta'_{\mathcal{R}} = \eta_{\mathcal{R}} \frac{1 + g(\mathcal{K})}{1 + 2\mathcal{K}[1 - g(\mathcal{K})]}. \quad (66)$$

The plots of three functions (66) are shown in figure 4. The dependence $\eta(\mathcal{K})$ is monotonous. Therefore smaller values of the purity parameter \mathcal{C} result in smaller values of η for a fixed value of the delta-potential strength \mathcal{Z} (except for the limit case of an impenetrable wall $\mathcal{Z} = \infty$). But two other dependences, $\eta_{\mathcal{R}}(\mathcal{K})$ and $\eta'_{\mathcal{R}}(\mathcal{K})$, are not monotonous. For this reason, highly mixed states with $\mathcal{C} \rightarrow 0$ may possess the same values of the conditional momentum transformation coefficients $\eta_{\mathcal{R}}$ and $\eta'_{\mathcal{R}}$ as pure states with $\mathcal{C} = 1$. However, the dependences of $\eta_{\mathcal{R}}$ (and especially $\eta'_{\mathcal{R}}$) on \mathcal{K} are rather weak, at least for $\mathcal{K} > 5$.

3.4. The invariant uncertainty product

When studying the evolution of wavepackets, it is a common practice to calculate the ‘uncertainty product’ $\sigma_x \sigma_p$ in order to estimate how close the packet is to the ‘minimal uncertainty state’. For example, a fast growth of this product was interpreted in [40] as an indication of the possibility of a ‘semiclassical chaos’ in quantum systems. As a matter of fact, it is better to use the *invariant uncertainty product* (IUP)

$$\Delta \equiv \sigma_x \sigma_p - \sigma_{xp}^2, \quad (67)$$

which is invariant with respect to arbitrary linear canonical transformations (in this subsection we use unscaled variables). The product (67) satisfies the Schrödinger–Robertson uncertainty relation $\Delta \geq \hbar^2/4$ [41–43]. Moreover, it does not depend on time for any *quadratic* Hamiltonian with arbitrary time-dependent coefficients, being the simplest example of the so-called universal quantum invariants [43–45]. For non-quadratic Hamiltonians (in particular, for the free motion in the half-space $x > 0$ with an impenetrable boundary at $x = 0$) the product (67), in general, depends on time. It was proposed in [46, 47] to use the rate of change of the function (67) (and of some other similar combinations) to classify the nonlinearities of quantum mechanical systems.

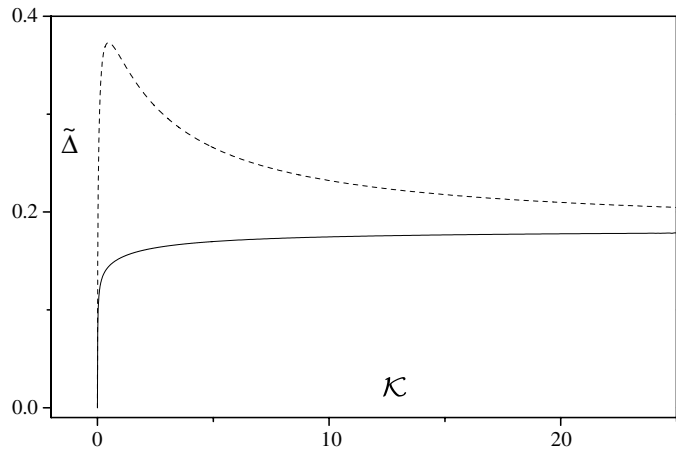


Figure 5. The asymptotical values of the normalized unconditional invariant uncertainty product $\tilde{\Delta}_\infty$ (68) (upper broken curve) and conditional invariant uncertainty product $\tilde{\Delta}_\mathcal{R}^\infty$ (69) (lower full curve) versus the dimensionless strength of the delta potential \mathcal{K} for the initial Gaussian packet (24).

Using equations (35)–(37), one can verify that asymptotically, as $t \rightarrow \infty$, the invariant uncertainty product (67) goes to a large constant value proportional to x_c^2 . Therefore it is convenient to introduce the dimensionless parameter $\tilde{\Delta} \equiv \Delta s^2 / (\hbar x_c)^2$. Its asymptotical value is (remember that $\mathcal{L} \leq 1/2$ for symmetrical initial states)

$$\tilde{\Delta}_\infty = \langle \tilde{k}^2 \rangle (1 - 4\mathcal{L}^2) - \langle \tilde{k}_\infty \rangle^2, \tag{68}$$

where \tilde{k} was defined in equation (25). Only in the case of $\zeta(k) = 2\mathcal{L} = 1$ does the right-hand side of (68) become zero. But this is the case of free motion, when Δ preserves its initial value (which does not depend on x_c , so that it looks like zero in the scale in which $x_c/s \gg 1$).

Equations (38)–(41) result in the following asymptotical constant value of the *conditional* IUP (remember that $\mathcal{R} \geq 1/2$ for symmetrical initial distributions):

$$\tilde{\Delta}_\mathcal{R}^\infty = \frac{1}{\mathcal{R}^2} [(2\mathcal{R} - 1)(\langle \tilde{k}_\infty^2 \rangle_\mathcal{R} - \langle \tilde{k}_\infty \rangle_\mathcal{R}^2) - (\langle \tilde{k}_\infty \rangle_\mathcal{R} - \langle \tilde{k}_\infty \rangle_\mathcal{W})^2]. \tag{69}$$

In figure 5 we show the dependences of the unconditional and conditional (normalized) IUPs $\tilde{\Delta}_\infty$ and $\tilde{\Delta}_\mathcal{R}^\infty$ on the dimensionless strength of the delta potential \mathcal{K} for the initial pure Gaussian packet (24). We see that two dependences are different, although they tend to the same limit value $\frac{1}{2}(1 - 2/\pi) \approx 0.18$ when $\mathcal{K} \rightarrow \infty$.

3.5. Reflection of ‘wide’ (shape-preserving) packets from the ideal wall

It seems worth giving an explicit example showing the qualitative difference between the reflection of ‘narrow’ and ‘wide’ packets. This can be done, for example, in the case of an ideal sharp boundary, when different families of exact solutions of the time-dependent Schrödinger equation can be constructed. One of these families consists of the following functions:

$$\Psi(x, t) = \frac{2x(m/\hbar)^{3/4}}{\pi^{1/4} \varepsilon^{3/2}} \exp\left[\frac{im\dot{\varepsilon}x^2}{2\hbar\varepsilon}\right], \tag{70}$$

where $\varepsilon(t)$ is a linear complex function of time:

$$\varepsilon(t) = b^{-1} + b(i + r)t, \quad -\infty < r < \infty. \tag{71}$$

The positive coefficient b determines the initial width of the wavepacket, whereas the parameter r is responsible for the initial correlation between the coordinate and momentum. The solutions in the form (70) were considered in [6], while their generalizations to a more general potential of the ‘singular oscillator’ with a time-dependent frequency were found in [48, 49].

For an arbitrary function $\varepsilon(t)$, the average values of the position and momentum operators, their products and squares in the state (70) are as follows:

$$\begin{aligned}\langle \hat{x} \rangle &= 2(\hbar/m\pi)^{1/2}|\varepsilon|, & \langle \hat{p} \rangle &= 2(\hbar m/\pi)^{1/2}\text{Re}(\dot{\varepsilon}\varepsilon^*)/|\varepsilon|, \\ \langle \hat{x}^2 \rangle &= 3\hbar|\varepsilon|^2/(2m), & \langle \hat{x}\hat{p} + \hat{p}\hat{x} \rangle &= 3\hbar\text{Re}(\dot{\varepsilon}\varepsilon^*), & \langle \hat{p}^2 \rangle &= 3\hbar m|\dot{\varepsilon}|^2/2.\end{aligned}$$

The specific feature of solution (70) is the conservation in time of the ratio of the coordinate dispersion to the average coordinate:

$$\xi = \sqrt{\sigma_x}/\langle \hat{x} \rangle = \sqrt{3\pi/8 - 1} \approx 0.42. \quad (72)$$

Hence the relative width of the packet (70) in the coordinate space is rather large, independently of the function $\varepsilon(t)$. The relative width of the packet in the momentum space, $\sqrt{\sigma_p}/\langle \hat{p} \rangle$, depends on time, but asymptotically, as $t \rightarrow \infty$, it goes to the same constant value ξ (72), if the function $\varepsilon(t)$ is given by equation (71). If $\langle \hat{p}(0) \rangle = 0$, then the momentum transformation coefficient equals $\eta = 8/(3\pi) \approx 0.85$.

The exact asymptotical (as well as the time-dependent) momentum probability density does not exhibit any oscillations (contrary to the case of initial narrow packets)

$$\tilde{\mathcal{P}}_\infty(P) = 4\pi^{-1/2}P^2 \exp(-P^2), \quad P > 0, \quad P = \frac{p}{b\sqrt{m\hbar}(1+r^2)}.$$

Moreover, the solution of the Schrödinger equation in the form of the shape-preserving wavepacket (70) possesses a *time-independent* universal uncertainty product

$$\Delta = \frac{3\hbar^2}{4\pi}(3\pi - 8) \approx 0.34\hbar^2$$

for any function $\varepsilon(t)$ (71).

4. Discussion

We have studied the influence of different factors on the reflection of narrow slow quantum packets from mirrors, having demonstrated that the form of the asymptotical momentum distributions depends crucially on the ratio of the initial mean momentum in the direction perpendicular to the surface of the mirror $|p_0|$ to the initial dispersion of this momentum component $\sqrt{\sigma_p(0)} \sim \hbar/s$, where s is the initial uncertainty in the position of the quantum particle (the centre of the wavepacket) in the perpendicular direction. If $|p_0| \gg \hbar/s$ (the case considered in most previous studies), then the asymptotical final momentum distribution is simply the initial one reflected from the point $p = 0$ in the momentum space (for $p_0 < 0$). But, if $|p_0| \ll \hbar/s$, then the form of the final momentum distribution is essentially different from the initial one. This results in a significant increase of the absolute value of the initial momentum in the direction perpendicular to the mirror, so that the asymptotical mean value p_∞ can become of the order of \hbar/s at the expense of ‘shrinking’ the momentum distribution. In a sense, an opposite effect, when the packet moving in the direction to the ‘mirror’ (created by the laser beam) ‘stops’ at the mirror, was discussed in [18]. However, this happens due to the entanglement between the internal and translational degrees of freedom of a cold atom, whereas the principal feature of the effect considered in our paper is its independence of the internal state of the atom (although the parameters of this state may enter implicitly in the potential responsible for the reflection).

We have shown that the concrete parameters of the mirror potential (such as the height V_0 and the characteristic width w) are not very crucial for the effect discussed: if V_0 is only a few times bigger than the characteristic energy of the packet $\hbar^2/(ms^2)$, then the properties of the reflected packet are close to those obtained in the approximation of an ideal impenetrable wall.

In the three-dimensional case the phenomenon can be interpreted as the effect of *quantum deflection* [22]. This effect, being almost trivial from the point of view of the theory of wavepacket propagation, nonetheless can serve as an impressive demonstration of the quantum nature of motion of ultraslow atoms. Indeed, let us make some evaluations, assuming that $p_0 = 0$. To prepare the initial state with the mean velocity directed along the surface and with a small uncertainty in the transverse position, one could use a long thin ‘atom waveguide’ [50], through which atoms could exit some trap where they have been cooled to the necessary low energy. Methods of generating arbitrary quantum states of the centre of mass motion of cold atoms have been proposed recently in [51]. The asymptotical mean value of the transverse velocity (in the direction perpendicular to the mirror) is $v_\infty \approx \hbar/(2ms)$. Taking $s = 10^{-6}$ cm, we obtain $v_\infty \sim 2$ cm s $^{-1}$ for Cs atoms and $v_\infty \sim 2$ m s $^{-1}$ for hydrogen atoms. The ‘deflection time’ equals, in order of magnitude, the time necessary to change the sign of the main part of the negative components of the initial momentum distribution. For the packet with the initial coordinate spread s , the most significant components in the momentum space are confined in the interval $|\delta p| \sim \hbar/s$, and they will reach the boundary by the time $mx_c/|\delta p|$, where $x_c \gg s$ is the initial distance from the mirror. Thus we can evaluate the ‘deflection time’ as $t_d \sim msx_c/\hbar$. Exact solutions for an ideal mirror considered in [22, 23] gave the same result, with the numerical factor 4 on the right-hand side. Taking $x_c = 1$ cm, which is quite a macroscopic parameter ($x_c/s \sim 10^6$), we have $t_d \sim 1$ s for Cs atoms and $t_d \sim 0.01$ s for hydrogen atoms. During this time the atom will pass about $2x_c$ in the parallel direction and about x_c in the perpendicular direction. If the initial mean velocity of the particle in the direction parallel to the mirror surface, v_\parallel , is of the same order of magnitude as v_∞ (which, in turn, is a typical velocity in experiments with ultracold atoms [52]), then a significant deflection can be quite observable. The effect is rather impressive from the classical point of view: a particle passes 1 cm from the wall: nonetheless, in the absence of any visible force, it ‘feels’ the presence of the boundary and changes the direction of motion by 45° (or even more, if the initial parallel velocity is less than v_∞). For light atoms, from H to Be, one can increase the initial distance even up to 10 cm.

Of course, there exist many difficulties which must be overcome in order to observe the effect of quantum deflection. Some of them were discussed in [22, 23]. Among the others, we can mention the broadening of the momentum distribution caused by spontaneous emission [53]. Here we would like to draw attention to several interesting theoretical problems emerging in connection with our study.

- (1) We have shown that the mean values of the momentum and other observables depend essentially on the experimental set-up, i.e. on the (im)possibility of observing the particle behind the mirror. However, all results have been derived under the condition of unitarity of evolution and its consequences, such as (3), (5) and (6). In real experiments with cold atoms, if an atom striking the mirror is not reflected from it, it will hardly pass through the mirror. Rather, it will be absorbed by it. Therefore, the case of *absorbing* atomic mirrors, when the evolution is *nonunitary*, deserves further study.
- (2) Studies of the nonunitary evolution seem to be important also from the point of view of the problems of damping (relaxation) and *decoherence* between different components of the packet. Indeed, the effect of deflection is a purely quantum one, because it is intimately

connected with the ‘wave’ properties of matter, or, better, with the existence of quantum interference phenomena. It is known, however, that the interaction with an ‘environment’ deteriorates the interference pictures. On the one hand, we have demonstrated that, for highly reflecting mirrors and Gaussian packets, the momentum transformation coefficient weakly depends on the degree of quantum purity, being practically the same for pure and highly mixed quantum states. Therefore, preparing the initial packet in a highly mixed state could give, in principle, some advantages, since one could start with a packet having larger spatial width than pure ones with the same initial energy. On the other hand, the interaction with an environment could cause the packet to spread faster than in the case of free (unitary) evolution, thus diminishing the energy of fluctuations and the mean momentum. The final effect depends, obviously, on the relations between the deflection time and the times of decoherence and relaxation (thermalization). The known experiments on the diffraction of atomic (electron, neutron, etc.) beams are in favour of the assumption that decoherence is not essential in this case (otherwise such experiments could not be performed). Moreover, there are models which show that, for instance, the decoherence time due to the interaction with cosmic background radiation is very large (exceeding the age of the universe) for microscopic quantum objects such as atoms [54]. However, many other possible mechanisms of decoherence and relaxation exist, as well as many different models describing these mechanisms. Therefore studies of such models taking account of reflection from boundaries could be interesting.

- (3) We have shown that, in the presence of the wall, the absolute value of the mean momentum of a particle is changed due to the deformation of the momentum distribution function. But the ideal wall is the limiting case of repulsive potentials. Hence one may suppose that the initial form of the wavepacket could be important in the processes of collisions between ultracold particles, when absolute values of their initial mean momenta are less or comparable with the square roots of the momenta dispersions. As a result of a distortion of the shapes of the particle wavepackets during the collision, the absolute values of the *mean momenta* will not be conserved. In this sense, the collisions between ultracold particles turn out to be inelastic, as far as the initial states are not idealized plane waves, but wavepackets of finite spatial extensions. This effect could be important for the physics of ultracold atoms (in this connection see also, for example, the recent papers [55]).
- (4) We have considered the effect of quantum deflection of *single atoms*. However, due to the fast development of the theory and experiments with beams of atoms in the state of the Bose–Einstein condensate (atomic lasers) [56], it would be interesting to see whether the effect of quantum deflection exists for such beams. In this case we have to deal with *nonlinear* modifications of the Schrödinger equation. Actually, the treatment of the effect in our paper is based essentially on the superposition principle for De Broglie’s waves, i.e. on the linearity of quantum mechanics. In the nonlinear case the situation could be quite different. For example, nonlinear equations admit *nonspreading beams* in free space. In such a case, one could suppose that no partial plane wave would reach the boundary to be reflected from it; hence no quantum deflection would occur. Indeed, it was shown recently [57] that the five-parameter family of the Stenflo–Sabatier–Doebner–Goldin *homogeneous* generalizations of the Schrödinger equation [58–61] contains a subfamily admitting the *finite-length soliton* solutions in the form (in the single space dimension, for simplicity)

$$\psi(x, t) = \{\cos[\gamma(x - kt)]\}^{1+\delta} e^{i(kx - \omega t)}, \quad |\gamma(x - kt)| < \pi/2,$$

whereas $\psi(x, t) \equiv 0$ if $|\gamma(x - kt)| \geq \pi/2$ and $\delta > 0$. These solutions are continuous and have continuous first derivatives. Other examples of equations admitting such

'compact ion' solutions were considered in [62]. Since these solutions are equal to zero identically outside some finite domain in the space, it is evident that any potential outside this domain will not affect these solutions. Studying the possibility of quantum deflection from mirrors for other kinds of nonlinear modifications of the Schrödinger equation, one could establish new bounds on the coefficients of these equations.

Acknowledgment

The authors acknowledge the full support of the Brazilian agency CNPq.

References

- [1] MacColl L A 1932 *Phys. Rev.* **40** 621
- [2] Hartman T E 1962 *J. Appl. Phys.* **33** 3427
- [3] Heller E 1975 *J. Chem. Phys.* **62** 1544
- [4] Hasse R W 1978 *J. Phys. A: Math. Gen.* **11** 1245
- [5] Andrews M 1981 *J. Phys. A: Math. Gen.* **14** 1123
- [6] Turner R E and Snider R F 1981 *Can. J. Phys.* **59** 457
- [7] Littlejohn R G 1986 *Phys. Rep.* **138** 193
- [8] Dodonov V V, Man'ko V I and Ossipov D L 1990 *Physica A* **168** 1055
- [9] Krause J L, Whitnell R M, Wilson K R, Yan Y J and Mukamel S 1993 *J. Chem. Phys.* **99** 6562
- [10] Bagrov V G, Belov V V and Trifonov A Y 1996 *Ann. Phys., NY* **246** 231
- [11] Brouard S and Muga J G 1998 *Phys. Rev. Lett.* **81** 2621
- [12] Doncheski M A and Robinett R W 1999 *Eur. J. Phys.* **20** 29
- [13] Weis J and Weis O 1999 *Eur. Phys. J. B* **12** 135
- [14] Petrillo V and Refaldi L 2000 *Opt. Commun.* **186** 35
- [15] Zhang W P and Walls D F 1993 *Phys. Rev. A* **47** 626
- [16] Deutschmann R, Ertmer W and Wallis H 1993 *Phys. Rev. A* **47** 2169
- [17] Adams C S, Sigel M and Mlynek J 1994 *Phys. Rep.* **240** 143
- [18] Pumares L, Plaja L, Roso L and Rzǎżewski K 1996 *Quantum Semiclass. Opt.* **8** 673
Roso L, Plaja L, Santos L, Pumares L and Rzǎżewski K 1998 *Opt. Commun.* **148** 376
- [19] Segev B, Côté R and Raizen M G 1997 *Phys. Rev. A* **56** R3350
Côté R, Segev B and Raizen M G 1998 *Phys. Rev. A* **58** 3999
- [20] Witte N S 1998 *J. Phys. A: Math. Gen.* **31** 807
- [21] Henkel C, Wallis H, Westbrook N, Westbrook C I, Aspect A, Sengstock K and Ertmer W 1999 *Appl. Phys. B* **69** 277
- [22] Dodonov V V and Andreato M A 2000 *Phys. Lett. A* **275** 173
- [23] Dodonov V V and Andreato M A 2002 *Laser Phys.* **12** 57
- [24] Landau L D and Lifshitz E M 1977 *Quantum Mechanics* (Oxford: Pergamon)
- [25] Faddeev L D 1958 *Dokl. Akad. Nauk* **121** 63
Faddeev L D 1958 *Sov. Phys.—Dokl.* **3** 747
- [26] Lamb G L Jr 1980 *Elements of Soliton Theory* (New York: Wiley)
- [27] Brouard S and Muga J G 1996 *Phys. Rev. A* **54** 3055
- [28] Erdélyi A (ed) 1953 *Bateman Manuscript Project: Higher Transcendental Functions* vol 2 (New York: McGraw-Hill)
- [29] Steinberg A M 1995 *Phys. Rev. A* **52** 32
- [30] Epstein P 1930 *Proc. Natl Acad. Sci. USA* **16** 627
- [31] Flügge S 1974 *Practical Quantum Mechanics* (Berlin: Springer)
- [32] Cook R and Hill R 1982 *Opt. Commun.* **43** 258
- [33] Balykin V I, Letokhov V S, Ovchinnikov Y B and Sidorov A I 1988 *Phys. Rev. Lett.* **60** 2137
- [34] Grimm R, Weidemüller M and Ovchinnikov Y B 2000 *Adv. At. Mol. Opt. Phys.* **42** 95
- [35] Gea-Banacloche J 2000 *Opt. Commun.* **179** 117
- [36] Mavromatis H A 1987 *Exercises in Quantum Mechanics* (Dordrecht: Reidel)
- [37] Manakov N L, Frolov M V, Starace A F and Fabrikant I I 2000 *J. Phys. B: At. Mol. Opt. Phys.* **33** R141
- [38] *Handbook of Mathematical Functions* 1974 ed M Abramowitz and I A Stegun (New York: Dover)
- [39] Gradshteyn I S and Ryzhik I M 1994 *Tables of Integrals, Series and Products* (New York: Academic)

- [40] Bonci L, Roncaglia R, West B J and Grigolini P 1992 *Phys. Rev. A* **45** 8490
- [41] Schrödinger E 1930 *Ber. Kgl. Akad. Wiss. Berlin* **24** 296
Robertson H P 1930 *Phys. Rev.* **35** 667
- [42] Dodonov V V, Kurmyshev E V and Man'ko V I 1980 *Phys. Lett. A* **79** 150
- [43] Dodonov V V and Man'ko V I 1989 *Invariants and the Evolution of Nonstationary Quantum Systems (Proc. Lebedev Physics Institute 183)* (Commack: Nova Science)
- [44] Dodonov V V and Man'ko V I 1985 *Group Theoretical Methods in Physics. Proc. 2nd Int. Seminar (Zvenigorod, Nov. 1982)* vol 1, ed M A Markov, V I Man'ko and A E Shabad (New York: Harwood Academic) p 591
- [45] Dodonov V V 2000 *J. Phys. A: Math. Gen.* **33** 7721
Dodonov V V and Man'ko O V 2000 *J. Opt. Soc. Am. A* **17** 2403
- [46] Dragt A J, Neri F and Rangarajan G 1992 *Phys. Rev. A* **45** 2572
- [47] Rivera A L, Atakishiyev N M, Chumakov S M and Wolf K B 1997 *Phys. Rev. A* **55** 876
- [48] Camiz P, Gerardi A, Marchioro C, Presutti E and Scacciatelli E 1971 *J. Math. Phys.* **12** 2040
- [49] Dodonov V V, Malkin I A and Man'ko V I 1974 *Physica* **72** 597
- [50] Ol'shanii M A, Ovchinnikov Y B and Letokhov V S 1993 *Opt. Commun.* **98** 77
Marksteiner S, Savage C M, Zoller P and Rolston S L 1994 *Phys. Rev. A* **50** 2680
Balykin V I 1999 *Adv. At. Mol. Opt. Phys.* **41** 181
Rohwedder B 2001 *Phys. Rev. A* **63** 053604
- [51] Olshanii M, Dekker N, Herzog C and Prentiss M 2000 *Phys. Rev. A* **62** 033612
- [52] Cohen-Tannoudji C N 1998 *Rev. Mod. Phys.* **70** 707
Weiner J, Bagnato V S, Zilio S and Julienne P S 1999 *Rev. Mod. Phys.* **71** 1
Wieman C E, Pritchard D E and Wineland D J 1999 *Rev. Mod. Phys.* **71** S253
Balykin V I, Minogin V G and Letokhov V S 2000 *Rep. Prog. Phys.* **63** 1429
- [53] Tan S M and Walls D F 1994 *J. Physique II* **4** 1897
- [54] de Oliveira M C, Almeida N G, Mizrahi S S and Moussa M H Y 2000 *Phys. Rev. A* **62** 012108
- [55] Kälbermann G 1999 *Phys. Rev. A* **60** 2573
Kälbermann G 2001 *J. Phys. A: Math. Gen.* **34** 3841
- [56] Courteille P W, Bagnato V S and Yukalov V I 2001 *Laser Phys.* **11** 659
- [57] Caparelli E C, Dodonov V V and Mizrahi S S 1998 *Phys. Scr.* **58** 417
- [58] Gradov O M and Stenflo L 1982 *Phys. Fluids* **25** 983
Malomed B A and Stenflo L 1991 *J. Phys. A: Math. Gen.* **24** L1149
- [59] Sabatier P C 1990 *Inverse Problems* **6** L47
Auberson G and Sabatier P C 1994 *J. Math. Phys.* **35** 4028
- [60] Doebner H-D and Goldin G 1992 *Phys. Lett. A* **162** 397
Doebner H-D and Goldin G 1994 *J. Phys. A: Math. Gen.* **27** 1771
- [61] Dodonov V V and Mizrahi S S 1993 *J. Phys. A: Math. Gen.* **26** 7163
Dodonov V V and Mizrahi S S 1995 *Ann. Phys., NY* **237** 226
- [62] Rosenau P and Hyman J M 1993 *Phys. Rev. Lett.* **70** 564
Dey B and Khare A 1998 *Phys. Rev. E* **58** R2741